Double Shock Control Bump Design Optimisation Using Hybridised Evolutionary Algorithms

D. S. Lee[1], L. F. Gonzalez[2], J. Periaux[1] and G. Bugeda[1]

[1]International Center for Numerical Methods in Engineering (CIMNE/UPC), Edificio C1, Gran Capitan, 08860, Barcelona Spain.
[2]Australian Research Centre Aerospace Automation (ARCAA) School of Engineering System, Queensland University of Technology, Australia.

***Abstract*—**The paper investigates the application of two advanced optimisation methods for solving active flow control device shape design problem and compares their optimisation efficiency in terms of computational cost and design quality. The first optimisation method uses Hierarchical Asynchronous Parallel Multi-Objective Evolutionary Algorithm (HAPMOEA) and the second uses Hybridized EA with Nash-Game strategies (Hybrid-Game). Both optimisation methods are based on a canonical evolution strategy and incorporate the concepts of parallel computing and asynchronous evaluation. One type of active flow control device named Shock Control Bump (SCB) is considered and applied to a Natural Laminar Flow (NLF) aerofoil. The concept of SCB is used to decelerate supersonic flow on upper/lower surface of transonic aerofoil that leads to a delay of shock occurrence. Such active flow technique reduces total drag at transonic speeds which is special interest to commercial aircraft.

Numerical results show that the Hybrid-Game helps an EA to accelerate optimisation process. From the practical point of view, applying a SCB on the suction and pressure sides significantly reduces transonic total drag and improves lift on drag (*L/D*) value when compared to the baseline design.

Keywords—Active Flow Control, Shock Control Bump, Shape design optimisation, Hybrid-Game, Nash Equilibrium, Evolutionary Algorithm.

1. Introduction

Developing an efficient optimisation technique is still one of the most challenging task in the field of Evolutionary Algorithms (EAs) research. As modern engineering problems become progressively more complex not only robust but also efficient tools are required. One of emerging techniques to improve an optimisation performance can be the use of Nash-equilibrium concept which will be acting as a pre-conditioner of global optimizer.

Lee et al. [1] studied the concept of Hybrid-Game (Pareto + Nash) coupled to a well-known MOEA; Non-dominating Sort Genetic Algorithm II (NSGA-II) [2] to solve Unmanned Aerial System (UAS) multi-objective Mission Path Planning System (MPPS) design problems. Their research shows that the Hybrid-Game improves the NSGA-II performance by 80% when compared to the original NSGA-II. In addition, Lee et al. [3] hybridised NSGA-II with Nash-Game strategy to study a role of Nash-Players in Hybrid-Game by solving multi-objective mathematical test cases; non-uniformly distributed non-convex, discontinuous and mechanical design problem. Their research also shows that Hierarchical Asynchronous Parallel Multi-Objective Evolutionary Algorithm (HAPMOEA) [4] can be also hybridised to solve a real-world robust multidisciplinary design problem. Numerical results show that the Hybrid-Game improves 70% of HAPMOEA performance while producing better Pareto optimal solutions. References [1, 3, 5] clearly describes merits of using Hybrid-Game coupled to MOEA for engineering design applications which consider a complex geometry or a large number of design variables.

Hybrid-Game has two major characteristics; the first is a decomposition of design problem, a multi-objective design problem for instance can be split into several simpler single-objective problems which correspond to Nash-Players which have their own design search space. The second temperament is that Nash-Players are synchronised with a Global/Pareto-Player as a pre-conditioner hence Pareto-Player can accelerate the optimisation process by using a set of elite designs obtained by the Nash-Players during optimisation.

The main goal of this paper is to investigate the efficiency of Hybrid-Game (Global + Nash) for a single-objective design problem. The search space herein will be decomposed to be explored by each Nash-Player. In this paper, HAMOPEA is hybridized with Nash game strategy to improve optimisation efficiency. Both optimisation methods are implemented to Active Flow Control (AFC) device shape design optimisation and their performance are compared in terms of computational cost and design quality.

Recent advances in design tools, materials, electronics and actuators offer implementation of flow control technologies to improve aerodynamic efficiency [6 -10]. Such aerodynamic improvement saves mission operating cost while condensing critical aircraft emissions. The main befits of using ACF techniques on current

transonic aircraft are to improve aerodynamic efficiency and reduce manufacturing cost when compared to designing a new airfoil or wing planform shape.

In this paper, one of active flow control devices; double Shock Control Bump (SCB) [8 -10] is applied on the suction and pressure sides of a Natural Laminar Flow (NLF) aerofoil; the RAE 5243 [10, 11] to reduce transonic total drag especially wave drag at the critical flight conditions where two shocks occur.

The rest of paper is organised as follows; Section 2 describes the optimisation methods; HAPMOEA and Hybrid-Game. Section 3 presents mathematical benchmarks using Hybrid-Game. Section 4 demonstrates the use of a SCB. Section 5 considers double SCB design optimisation using HAPMOEA and Hybrid-Game. Section 6 delivers conclusion and future works.

2. Optimisation Methods

The evolutionary algorithm used in this paper is based on Covariance Matrix Adaptation Evolutionary Strategies (CMA-ES) [12, 13] which incorporates an asynchronous parallel computation and a Pareto tournament selection [14 -16]. The first method; HAPMOEA uses the concept of hierarchical multi-population topology which can handle different models including precise, intermediate and approximate models. Each node (Node0 ~ Node6) belonging to the different hierarchical layer can be handled by a different EA code as shown in Figure 1 (a).

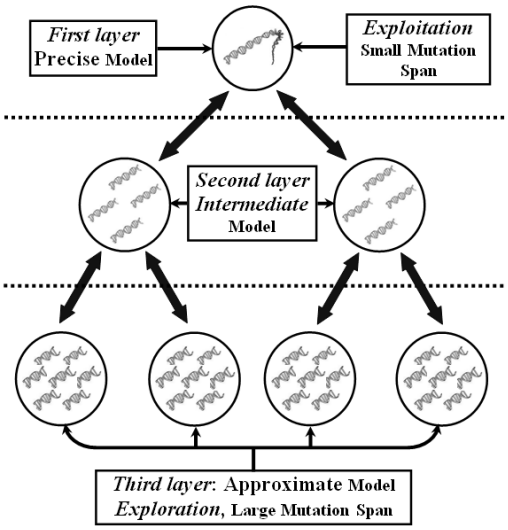

Figure 1 (a). Hierarchical multi-population topology.

The second method hybridises HAPMOEA by applying a concept of Nash-Equilibrium instead of the concept of hierarchical multi-population topology [4, 17] which is denoted as Hybrid-Game. Figure 1 (b) shows one example topology for Hybrid-Game which consists of three Nash-Players and one Global-Player. The Nash-Game players choose their own strategy to improve their own objective. The Hybrid-Game takes a high fidelity/resolution population from HAPMOEA to the core of Nash-Game hence; the Nash-Players can seed/update their elite designs to Global-Player (Node0).

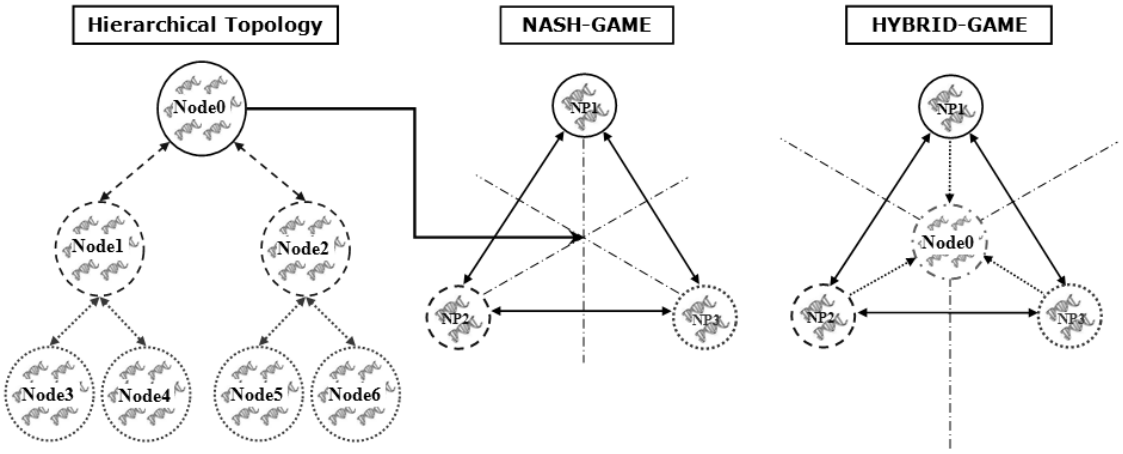

Figure 1 (b). Example topology of Hybrid-Game.

Both HAPMOEA and Hybridised EA are coupled to the aerodynamic analysis tool. Details and validations of HAPMOEA and Hybrid-Game can be found in references [1, 3, 17]. Lee et al. [3, 17] described the details of topology for HAPMOEA and Hybrid-Game for robust multidisciplinary design problem, and showed their validation by solving multi-objective mathematical design problems including non-uniformly distributed non-convex, discontinuous (TNK), mechanical design problems.

3. Mathematical Benchmarks

In this section, Hybrid-Game is implemented to NSGA-II [2] to solve two complex mathematical design problems; single-objective mathematical design developed by author and Zitzler, Deb and Thiele (ZDT6) [18] are considered. Both NSGA-II and Hybrid-Game use same optimization parameters; a constant random seed, population size = 100, crossover rate = 0.9 and mutation probability = $1/n$ where n is the number of decision variables. The reason why a constant random seed is considered is to produce the same initial random population for both NSGA-II and Hybrid-Game.

3.1. Single-objective Mathematical Design Optimisation using NSGA-II and Hybrid-Game

One single-objective mathematical design problem which is similar to inverse design (desired to have zero value for fitness function) is considered. The fitness function is shown (1). Two test cases are conducted with different number of design variables (n = 20, n = 30). The same random initial population is used for both NSGA-II and Hybrid-Game. Hybrid-Game employs three players; one Global-Agent (GlobalP) minimising (1) and two Nash-Agents (NashP1, NashP2) misimising (2) and (3). The stopping criterion for NSGA-II and Hybrid-Game is when the fitness value reaches lower than predefined value 1.0×10^{-6} i.e. f_{RMOGA} and $f_{HRMOGA} \leq 1.0 \times 10^{-6}$.

$$f_{Global-Player}\left(x_i\right) = \sum_{i=2}^{n}\left(x_i - 0.5\right)^2 \tag{1}$$

$$f_{Nash-Player1}\left(x_i, x_i^*\right) = \sum_{i=1}^{n_{NashP1}}\left(x_i - 0.5\right)^2 + \sum_{i=1}^{n_{NashP2}}\left(x_i^* - 0.5\right)^2 \tag{2}$$

$$f_{Nash-Player2}\left(x_i^*, x_i\right) = \sum_{i=1}^{n_{NashP1}}\left(x_i^* - 0.5\right)^2 + \sum_{i=1}^{n_{NashP2}}\left(x_i - 0.5\right)^2 \tag{3}$$

where n_{Global} = [20,30], n_{NashP1} = [10,15], n_{NashP2} = [10,15]. x_i* is an elite design obtained by the Nash-Player 1 and Nash-Player 2.

Figure 2 compare the convergence history obtained by NSGA-II and Hybrid-Game for (n = 20, n = 30). It can be seen that Hybrid-Game has converged ($f \leq 1.0 \times 10^{-6}$) faster than NSGA-II; for 20 design variables, Hybrid-Game converged after 12,058 function evaluations (4.3 seconds) while NSGA-II converged after 31,262 function evaluations (8.0 seconds). For the second test with 30design variables, Hybrid-Game converged after 21,101 function evaluations (10.178 seconds) while NSGA-II converged after 56,961 function evaluations (20.975 seconds). It can be seen that Hybrid-Game can save almost 50% of computational cost while converging at one third of total function evaluations of NSGA-II.

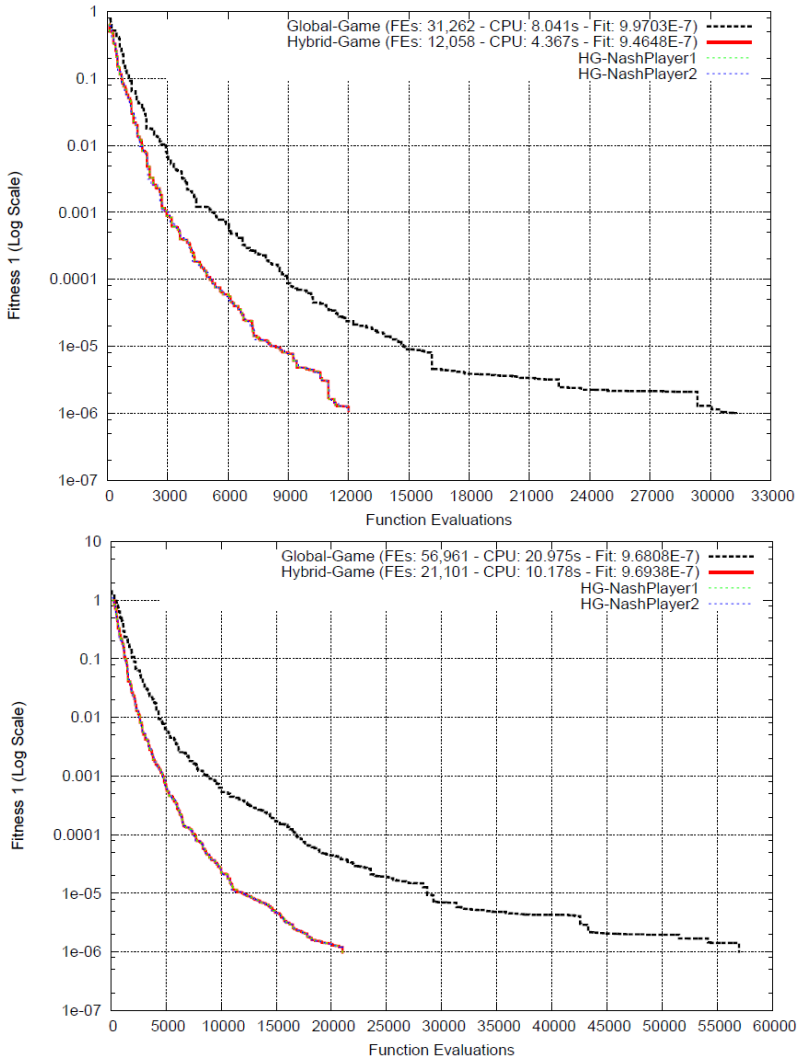

Fig. 2. Convergence history obtained by NSGA-II and Hybrid-Game for Test1 (n_{Global} = 20: top) and Test2 (n_{Global} = 30: bottom).

3.2. Multi-objective Mathematical Design Problem using NSGA-II and Hybrid-Game

For the multi-objective mathematical design, ZDT6 is considered. It is formulated as shown in Equations (1) and (2) [18].

$$f_1(x_1) = 1 - \exp(-4x_1)\sin^6(6\pi x_1) \tag{1}$$

$$f_2(f_1, g) = 1 - (f_1/g)^2 \tag{2}$$

where $m = 10$, $x_i \in [0,1]$ and $g(x_{i,\ldots,m}) = 1 + 9\left(\left(\sum_{i=2}^{m} x_i\right)\Big/(m-1)\right)^{0.25}$.

NSGA-II itself has one population considering both Equations (1) and (2) while Hybrid-Game employs two more populations; Nash-Player 1 considers minimisation of Eq. (1) as its sole objective while Nash-Player 2 considers minimisation of Eq. (2) with fixed elite design x_1* as shown in Equation (3).

$$f_{NP2}(f_{NP1}, g) = 1 - \left(f_{NP1}(x_1^*)/g\right)^2 \tag{3}$$

In this problem, Nash-Game splits the ZDT6 into two simpler problems corresponding to Nash-Player 1 and Nash-Player 2. In addition, the elite designs; here x_1*,.., x_{10}* obtained by Nash-Players 1 and 2 will be seeded to the Pareto-Player population (original population of NSGA-II). Due to the constant random seed, NSGA-II and

Hybrid-Game produce the same initial random population as shown in Figure 3. In addition, the optimisation using NSGA-II is stopped after 200 generations while Hybrid-Game is stopped when Hybrid-Game reached the computational cost of NSGA-II. These conditions will provide to make a fair comparison.

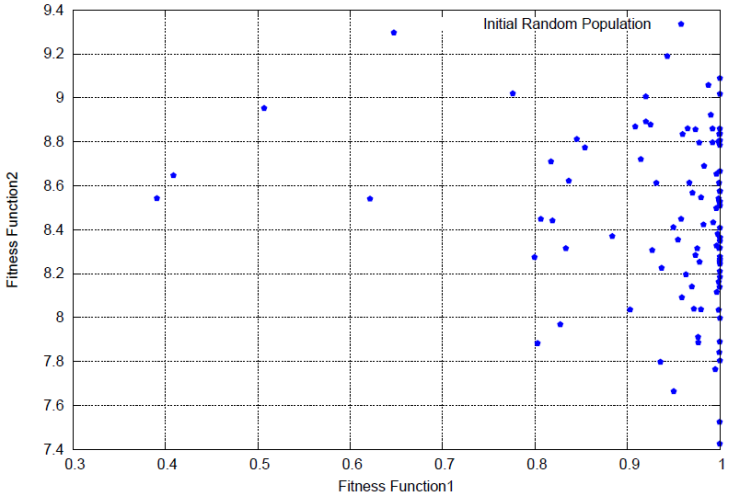

Fig. 3. Initial random population for ZDT6 obtained by NSGA-II and Hybrid-Game.

Pareto optimal fronts obtained by NSGA-II (after 100 and 200 generations) and Hybrid-Game (after 5 and 13 seconds) are compared as shown in Figures 4 (a) and 4 (b). It can be seen that both NSGA-II and Hybrid-Game are converging to the same solutions however the Pareto-Game of Hybrid-Game has much better solutions for both objectives after 100 and 200 generations when compared to NSGA-II. This is because the Nash-Players are acting as pre-conditioners to the Pareto-Player.

Table 1 compares the fitness values obtained by NSGA-II (after 100 and 200 generations) and Hybrid-Game (after 5 and 13 seconds). The best solutions obtained by Hybrid-Game are better than NSGA-II due to injection of the elite design obtained by Nash-Game to the Pareto-Game population of Hybrid-Game. In other words, the use of Hybrid-Game (Nash + Pareto) improves the optimisation efficiency of NSGA-II due to the two major characteristics; the decomposition of design problem and the pre-conditioning.

Table 1. Comparison of fitness values obtained by NSGA-II and HNSGA-II for ZDT6.

Optimiser	NSGA-II	Hybrid-Game (HNSGA-II)		
Game Strategies	Pareto-Game	Pareto-Game	Nash-Game	
			Nash-Player1	Nash-Player2
Best Fit1 (Gen100)	0.38832, 1.27476	*0.38832, 1.11518*	*0.38832*	*0.97123*
Best Fit2 (Gen100)	0.99790, 0.56306	*0.99957, 0.27448*		
Best Fit1 (Gen200)	0.38832, 0.88232	*0.38832, 0.85884*	*0.38832*	*0.85296*
Best Fit2 (Gen200)	0.99999, 0.03730	*0.99999, 0.01392*		

Note: Best Fit1 and Fit2 represent the best solutions for fitness function 1 and 2 respectively.

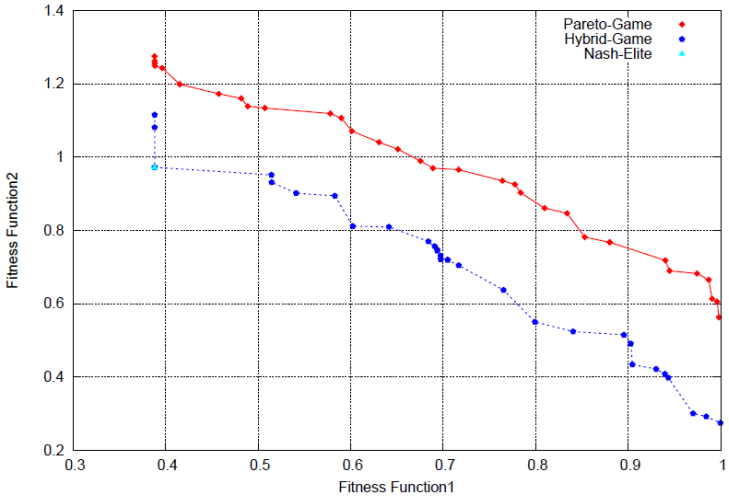

Fig. 4 (a). Pareto optimal front obtained by NSGA-II (100 generations, elapsed time: 5 seconds) and Hybrid-Game (89 generations).

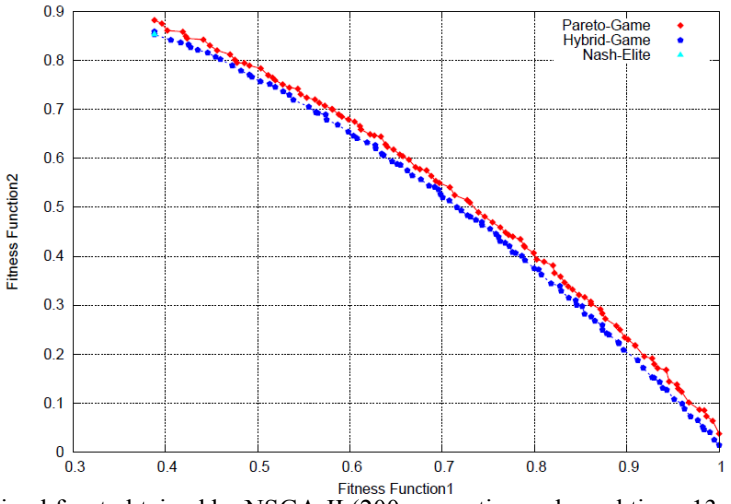

Fig. 4 (b). Pareto optimal front obtained by NSGA-II (200 generations, elapsed time: 13 seconds) and Hybrid-Game (160 generations).

4. Wave Drag Reduction via. Shock Control Bump

At transonic speed, the flow over aircraft wing causes shock waves where there is a large amount of gas property changes and the flow becomes irreversible. Through the shock, total pressure decreases and entropy increases which means there is a loss of energy. In other words, there is an increment of wave drag. To cope with this problem, Ashill *et al*. 1992 [7] proposed the concept of a transonic bump which so-called Shock Control Bump (SCB) by using geometry adaption on an aerofoil. As illustrated in Figure 5, the typical design variables for SCB are: length, height and peak position and, the center of SCB will be located at sonic point where the flow speed transits from supersonic to subsonic on the transonic aerofoil design.

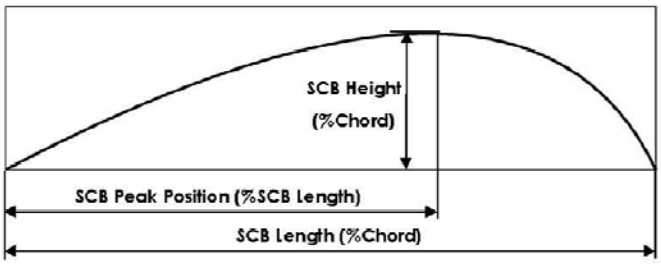

Fig. 5. Design components of Shock Control Bump.

Figure 6 illustrates the *Cp* distributions obtained by RAE 2822 aerofoil and RAE 2822 with SCB. For aerodynamic analysis tool, MSES (Euler and Boundary layer) written by Drela [19] is utilised. The transonic flow over normal aerofoil without SCB accelerates to supersonic and the pressure forms a strong shock that leads a high wave drag (Cd_{Wave}) however the pressure difference over the SCB causes a deceleration of supersonic flow which delays shock occurrence. SCB cannot totally remove a shock however it makes a weaker shock or breaks into isentropic compression waves (lower Cd_{Wave}).

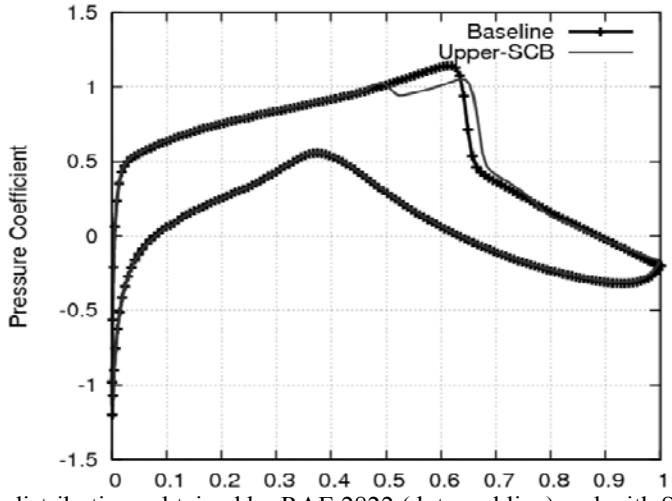

Fig. 6. *Cp* distributions obtained by RAE 2822 (dots and line) and with SCB (line).

Table 2 compares the aerodynamic performance obtained by RAE 2822 and with SCB. Even though applying SCB on RAE 2822 produces 5% higher viscous drag ($\Delta Cd_{Viscous}$ = 0.0005), it reduces 60% wave drag (ΔCd_{Wave} = 0.0036) while improving 19% of *L/D* when compared to RAE 2822 aerofoil.

Table 2. Aerodynamic Characteristics

Aerofoil	Cd_{Total}	$Cd_{Viscous}$	Cd_{Wave}	*L/D*
RAE 2822	0.0153	0.0093	0.0060	34.34
with SCB	0.0123 (-20%)	0.0098 (+5%)	0.0024 (-60%)	42.6 (+24%)

Note: M_∞ = 0.77, Re = 17.93 $\times 10^6$ and *Cl* is fixed to 0.524.

Applying SCB on either upper or lower surface of aerofoil will produces slightly thicker thickness ratio (*t/c*) which causes increment of viscous drag ($Cd_{Viscous}$) however the use of SCB is still beneficial due to Cd_{Wave} reduction especially when the Mach number is higher than critical Mach number where the shock starts appearing.

In Section 5, the shape of SCB is optimized at critical flight conditions where two shocks occur on the suction and pressure sides of aerofoil. This flight conditions make a suitable application for Hybrid-Game (Global + Nash) since two SCBs are required. The aerodynamic characteristics of baseline with the optimal double SCB are also investigated at normal flight conditions where a single shock is on the upper surface of aerofoil.

5. SCB Design Optimisation on RAE5243

For baseline design, a natural laminar flow aerofoil RAE 5243 is selected as shown in Figure 7 (a). The problem considers the critical flow conditions; M_∞ = 0.8, C_l = 0.175, *Re* = 18.63 $\times$ 10^6 where two shocks occur on the suction and pressure sides of RAE 5243 aerofoil as shown in Figure 7 (b).

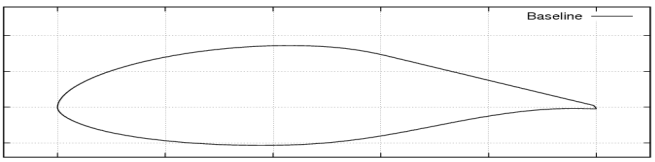

Fig. 7 (a). Baseline design (RAE 5243) geometry (Note: max *t/c* = 0.14 at 41%c and max camber = 0.018 at 54%c).

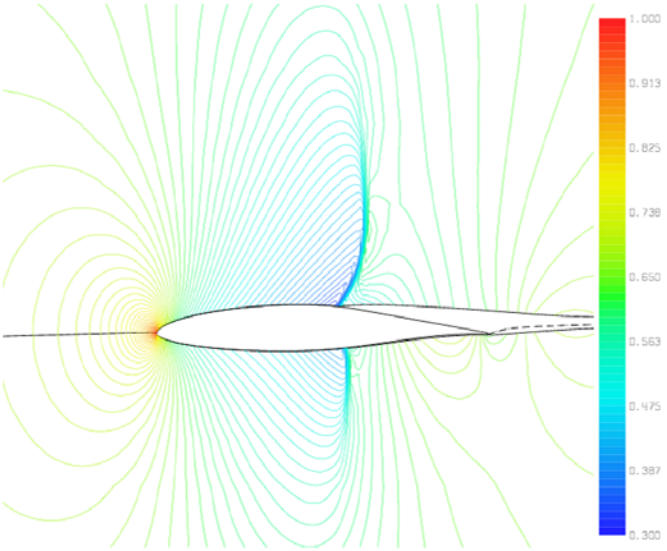

Fig. 7 (b). P/P_0 contour of RAE 5243.

The upper and lower sonic points are occurred at 62.6% and 58.1% of chord respectively. In following sections, double SCB design optimization using HAPMOEA and Hybrid-Game are conducted to minimize the total drag (Cd_{Total}). The aerodynamic analysis tool; MSES will run two times at each function evaluation; the first run will analyse upper SCB and then upper and lower SCB will be analysed at the second run.

5.1 Evaluation Mechanism for HAPMOEA and Hybrid-Game

Figure 8 (a) shows the evaluation mechanism for HAPMOEA which consists of hierarchical multi-population (Node 0 ~ Node 6) based on multi-resolution. Each population will run aerodynamic analysis tool two times to evaluation double SCB design in different resolution conditions.

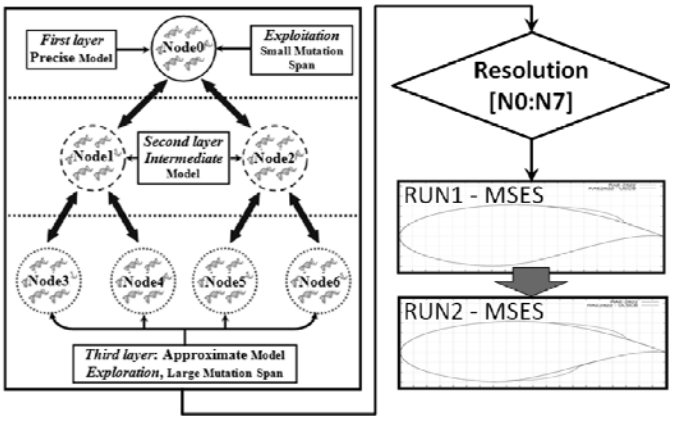

Fig. 8 (a). Evaluation mechanism of HAPMOEA.

Figure 8 (b) shows the evaluation mechanism for Hybrid-Game which employs three players; Global-Player and Nash-Player 1 and 2. Solely Global-Player runs aerodynamic analysis tool two times since its optimisation domain includes both upper and lower SCB. However, the analysis tool will run only once for Nash-Player 1 and 2 due to the Nash-Game characteristics; decomposition of design problem. For Hybrid-Game, double SCB design problem becomes two single SCB design problems; Nash-Game 1 will only optimize upper SCB with elite lower SCB obtained by Nash-Player 2 while Nash-Player 2 will optimise lower SCB with elite upper SCB design from Nash-Player 1. The elite designs obtained by Nash-Players will be seed to the population of the Global-Player that will allow Global-Player to accelerate optimisation process.

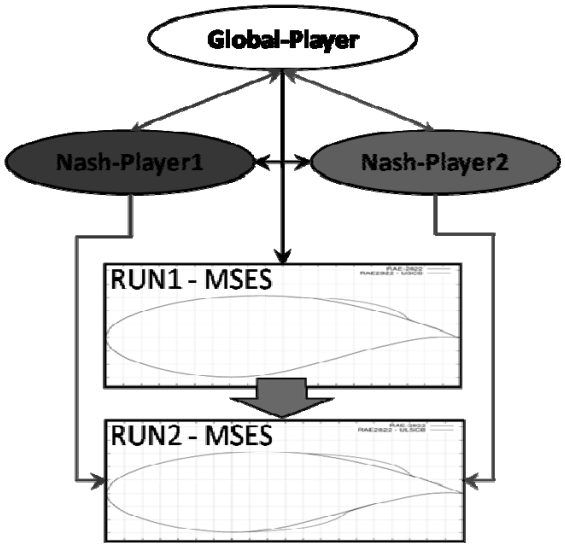

Fig. 8 (b). Evaluation mechanism of Hybrid-Game.

5.2 SCB Design Optimisation using HAPMOEA

Problem Definition

This test case considers a single objective double SCB design optimisation using HAPMOEA to minimize total drag (Cd_{Total}) which consists of viscous drag ($Cd_{Viscous}$) and wave drag (Cd_{Total}). The flow conditions M_∞ = 0. 8, C_l = 0.175, Re = 18.63 × 10^6. The fitness function is shown in Eq. (4).

$$f\left(U\_SCB, L\_SCB\right) = \min\left(Cd_{Total}\right) \tag{4}$$

where $Cd_{Total} = Cd_{Viscous} + Cd_{Wave}$.

Design Variables

The design variable bounds for both SCB on the suction and pressure sides are illustrated in Table 3. In total, six design variables are considered for double SCB.

Table 3. SCB Design Variables and Bounds

Design Variables	Lower bound	Upper bound
Length (% chord)	15	30
Height (% chord)	0.15	0.65
Peak position	0	100

Note: Peak position is in % of SCB length.

The centre of SCB (50% of SCB length) will be positioned where the flow speed transits from supersonic to subsonic.

Implementation

The following conditions are for multi-resolution/population hierarchical populations.

- 1st Layer: Population size of 10 with a computational grid of 36 × 213 points (Node0).
- 2nd Layer: Population size of 20 with a computational grid of 24 × 131 points (Node1, Node2).
- 3rd Layer: Population size of 20 with a computational grid of 36 × 111 points (Node3 ~ Node6).

Note: these grid conditions produce less than 5% accuracy error compared to precise model at the 1st layer (Node0).

Numerical Results

As illustrated in Figure 9, the algorithm was allowed to run for 24 hours and 2,508 function evaluations using a single 4 × 2.8 GHz processor and convergence occurred at 1,053 function evaluations with Cd_{Total} = 0.03441 after ten hours.

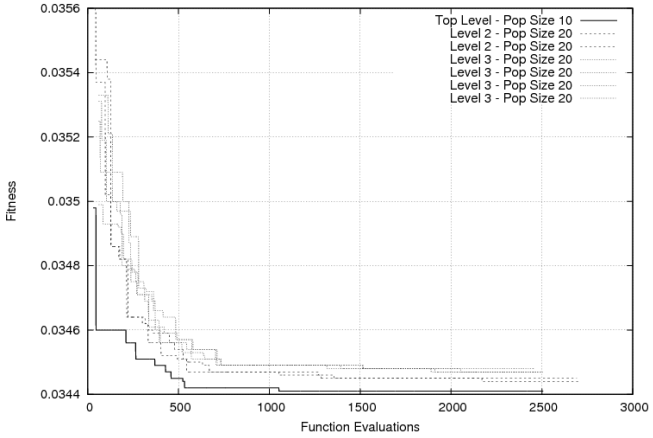

Fig. 9. Convergence objective using HAPMOEA.

Table 4 compares the aerodynamic characteristics obtained by the baseline design (RAE 5243) and the baseline design with upper and lower SCBs. Applying SCB on upper surface of RAE 5243 aerofoil saves the wave drag by 8% which leads 12% of total drag reduction. This optimal double SCB improves *L/D* by 13.0%.

Table 4. Aerodynamic Characteristics.

Aerofoil	Cd_{Total}	Cd_{Wave}	*L/D*
Baseline	0.03898	0.0088	4.49
with SCB	0.03442 (- 12%)	0.0081 (-8%)	5.08 (+ 13%)

Note: *Cl* is fixed to 0.175.

The optimal shape of double SCB is described in Table 5. Figure 10 compares the geometry of the baseline design and baseline with the optimal double SCB which has same *t/c* while the max camber is increased by 0.0005 and its position is moved 16%c towards to the trailing edge when compared to the baseline design.

Table 5. Optimal Double SCB Design Components.

Variables	*Length (%c)*	*Height (%c)*	*Peak Position*
U_SCB	23.31	0.649	84.95
L_SCB	26.38	0.477	75.98

Note: *Peak position* is in % of SCB length. The U_SCB starts from *x* and *y* coordinates (0.5084, 0.0838) to (0.7416, 0.0480) and L_SCB is positioned from (0.4397, -0.05269) to (0.7035, -0.0258).

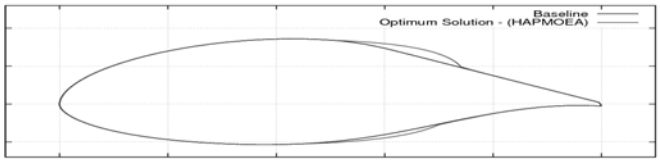

Fig. 10. Baseline design with the optimal double SCB obtained by HAPMOEA (Note: max *t/c* = 0.14 at 41%c and max camber = 0.0209 at 69.8%c).

Figure 11 shows the contour of baseline design with the optimal double SCB. It can be seen that the strong shocks on the baseline design shown in Figure 7 b) get weaker by adding double SCB.

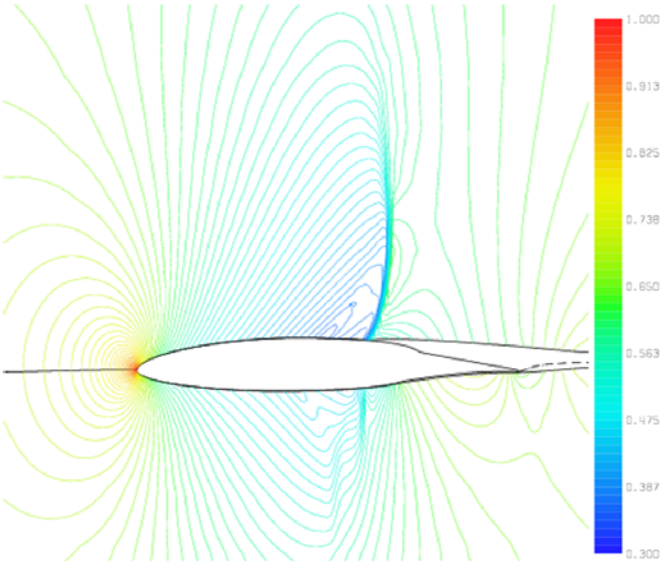

Fig. 11. P/P_0 contour of the optimal double SCB solution obtained by HAPMOEA.

Figure 12 compares *Cp* distribution obtained by the baseline design and the baseline design with upper and lower SCB. It can be seen that the total drag is reduced by 9% while the double SCB reduces 12% of total drag. The shock on upper surface is delayed while the shock on lower surface becomes weak isentropic waves.

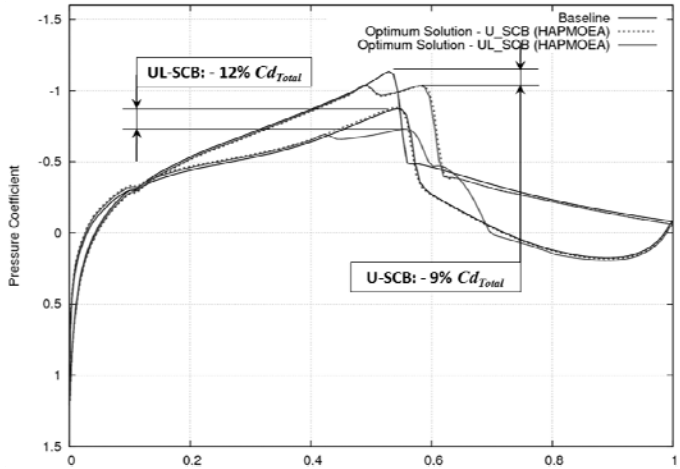

Fig. 12. *Cp* distributions obtained by baseline (black line) and the optimal solution (broken line: only upper SCB, red line: upper and lower SCBs).

5.3 SCB Design Optimisation using Hybrid-Game

Problem Definition

This test case considers a single objective double SCB design optimisation using Hybrid-Game on MOEA to minimize total drag at flow conditions $M_\infty = 0.8$, $C_l = 0.175$, $Re = 18.63 \times 10^6$. Hybrid-Game consists of three players; one Global-Player (*GP*), two Nash-Players (*NP1* and *NP2*) instead of hierarchical multi-population/resolution (Node 0 ~ Node 6). The fitness functions for Hybrid-Game are shown in Eq. (5).

$$\begin{aligned} f_{GP}\left(U\_SCB, L\_SCB\right) &= \min\left(Cd_{Total}\right) \\ f_{NP1}\left(U\_SCB, L\_SCB*\right) &= \min\left(Cd_{Total}\right) \\ f_{NP2}\left(U\_SCB*, L\_SCB\right) &= \min\left(Cd_{Total}\right) \end{aligned} \tag{5}$$

where $Cd_{Total} = Cd_{Viscous} + Cd_{Wave}$. *U_SCB* and *L_SCB* represent upper and lower SCB, and * is elite SCB design obtained by Nash-Players. *U_SCB** and *L_SCB** are elite SCB designs obtained by Nash-Player 1 and 2. These elite SCB designs will be seeded to the population of Global-Player at every 10 function evaluations and will act as a pre-conditioner.

Design Variables

The design variable bounds for the upper and lower SCB geometry are illustrated in Table 3. Table 6 shows design variable distribution for Hybrid-Game. It can be seen that the Nash-Players 1 and 2 consider only 3 design variables while the Global-Player of Hybrid-Game considers 6 design variables.

Table 6. Design Variable Distribution for Hybrid-Game.

Type of SCB	Hybrid-Game			HAPMOEA (Node 0 ~ 6)
	GP	*NP1*	*NP2*	
U_SCB	√	√		√
L_SCB	√		√	√

Note: *GP, NP1 and NP2* represent global player and Nash-Players 1 and 2.

Implementation

The following conditions are for Hybrid-Game; Global-Player, Nash-Player 1 and Nash-Player 2.

- GP: Population size of 10 with a grid of 36 × 213.
- NP1: Population size of 10 with a grid of 36 × 213.
- NP2: Population size of 10 with a grid of 36 × 213.

Numerical Results

As illustrated in Figure 13, the algorithm was allowed to run for 5 hours and 1,775 function evaluations using single 4 × 2.8 GHz processor and convergence occurred at 683 function evaluations (approximately 1.9 hours) with Cd_{Total} = 0.0344 which HAPMOEA could not capture even after 24 hours shown in previous test Section B. To compare the computational efficiency of HAPMOEA and Hybrid-Game, the fitness value is chosen to Cd_{Total} = 0.03441 which HAPMOEA captured after 10 hours. Hybrid-Game took 1.48 hours which is only 15 % of HAPMOEA computational cost. In other words, Nash-Game improves performance of EA by 85% as shown in Figure 14.

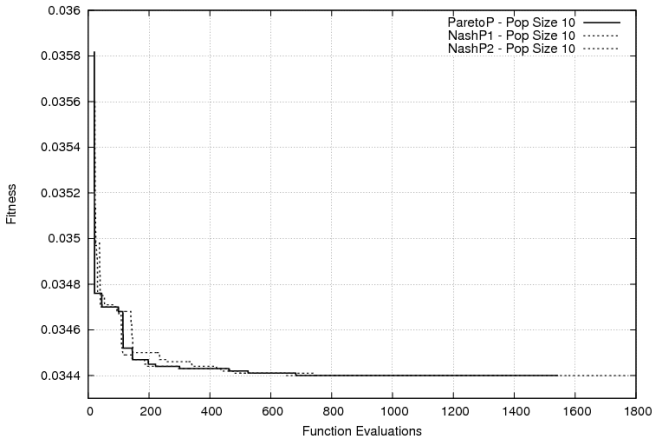

Fig. 13. Convergence objective using Hybrid-Game.

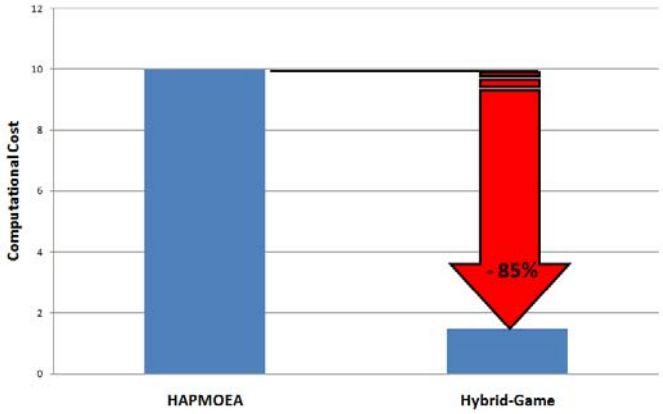

Fig. 14. Performance comparison between HAPMOEA and Hybrid-Game.

Table 7 compares the aerodynamic characteristics obtained by the baseline design (RAE 5243) and the baseline design with upper SCB. Applying SCB on upper surface of RAE 5243 aerofoil saves the wave drag by 8% which leads 12% of total drag reduction. This optimal double SCB improves *L/D* by 13.0%.

Table 7. Aerodynamic Characteristics.

Aerofoil	Cd_{Total}	Cd_{Wave}	*L/D*
Baseline	0.03898	0.0088	4.49
with SCB	0.03437 (- 12%)	0.0081 (-8%)	5.09 (+ 13%)

Note: *Cl* is fixed to 0.175.

The optimal double shape of double SCB obtained by Hybrid-Game is described in Table 8. It can be seen that the upper SCBs obtained by Hybrid-Game and HAPMOEA (Table 5) have almost same shape while the lower SCB from Hybrid-Game is 10% shorter than the lower SCB obtained by HAPMOEA.

Table 8. Optimal SCB Design Variables obtained by Hybrid-Game.

Variables	*Length (%c)*	*Height (%c)*	*Peak Position*
U_SCB	23.65	0.649	84.99
L_SCB	23.88	0.384	80.35

Note: *Peak position* is in % of SCB length. U_SCB and L_SCB represent SCB on the suction and pressure sides of RAE 5243 aerofoil. The U_SCB starts from *x* and *y* coordinates (0.5067, 0.0839) to (0.7432, 0.04774) and L_SCB position is located from (0.4521, -0.0528) to (0.6910, -0.0277).

Figure 15 illustrates the geometry of the baseline design and baseline with the optimal double SCB from HAPMOEA and Hybrid-Game. The baseline design with double SCB obtained by Hybrid-Game has same *t/c* while the max camber is increased by 0.00055 and its position is moved 15%c towards to the trailing edge when compared to the baseline design.

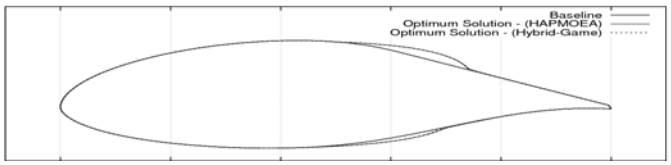

Fig. 15. Baseline design with the optimal double SCB (Note: max *t/c* = 0.14 at 41%c and max camber = 0.0214 at 69.0%c).

Figure 16 shows the pressure contour of baseline design with the optimal double SCB obtained by Hybrid-Game. It can be seen that the upper shock is moved toward to the trailing edge while lower shock becomes weak isentropic waves.

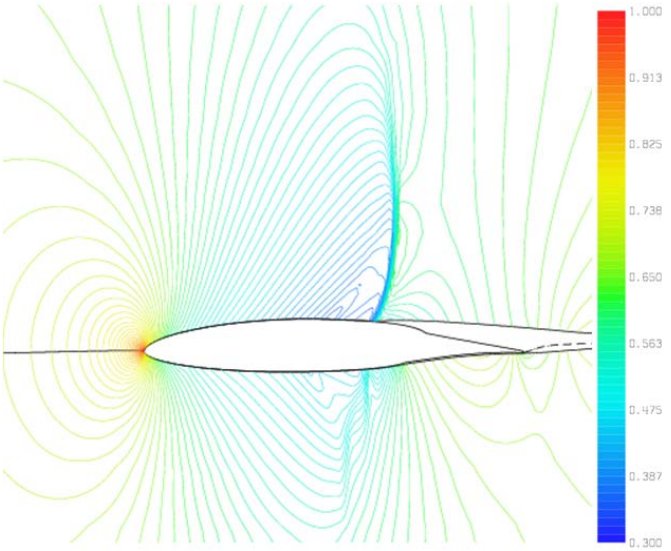

Fig. 16. P/P_0 contour of the optimal double SCB solution obtained by Hybrid-Game.

Figures 17 (a) and 17 (b) compare a total drag (Cd_{Total}) and a wave drag (Cd_{Wave}) distributions obtained by the baseline design and with the optimal double SCB from both HAPMOEA and Hybrid-Game. The flow conditions are $M_\infty \in [0.5{:}0.85]$ with constant $Cl_{Fixed} = 0.175$ and $Re = 18.63 \times 10^6$. It can be seen that both optimal double SCB obtained by HAPMOEA and Hybrid-Game perform almost same drag along the Mach numbers. The baseline design with the optimal double SCB starts to produce lower total drag when Mach number is higher than 0.71. One thing should be noticed from Figure 17 b) is that the critical Mach number ($M_C = 0.65$) for baseline design is extended to 0.71 by adding double SCB. The maximum total drag reduction (-26%) is observed at $M_\infty = 0.75$ shown in Figure 17 (a) due to 88% of wave drag reduction shown in Figure 17 (b) when compared to the baseline design.

The optimal double SCB obtained by HAPMOEA and Hybrid-Game is also tested at five different flight conditions. The histogram showed in Figure 18 (a) compares the total drag. It can be seen that the double SCB optimized at critical flight conditions reduces more total drag by 15 to 44% while improving the lift to drag ratio by 13.5 to 80% as shown in Figure 18 (b) at the normal flight conditions.

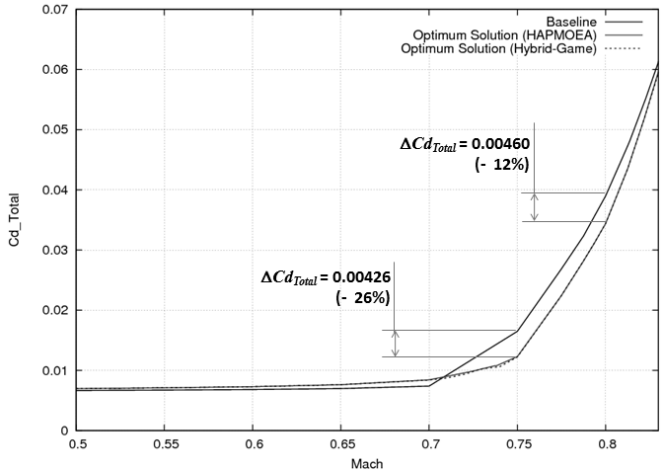

Fig. 17 (a). Cd_{Total} vs. Mach numbers.

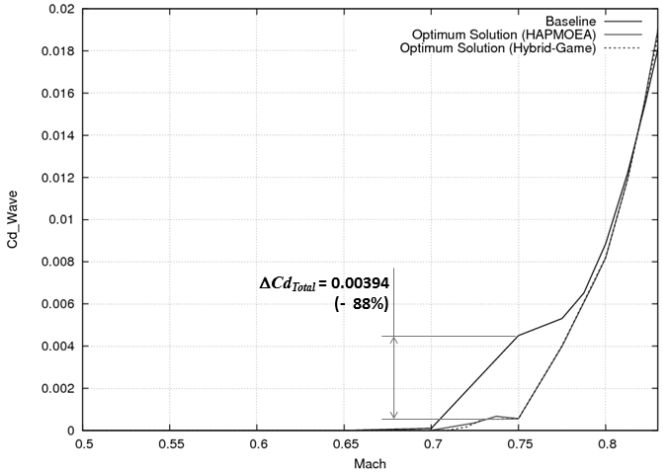

Fig. 17 (b). Cd_{Wave} vs. Mach numbers.

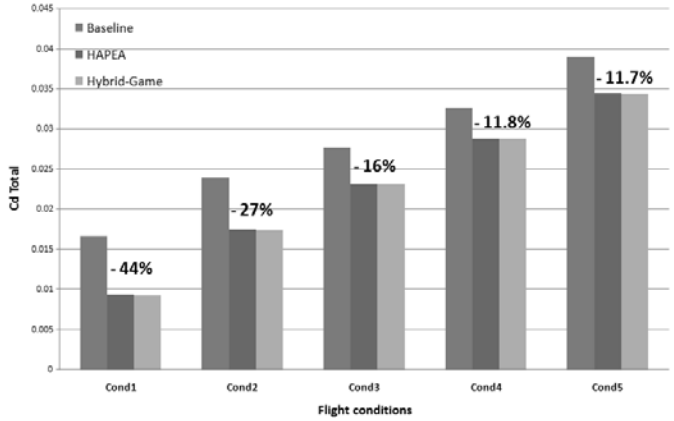

Fig. 18 (a). Drag reduction obtained by the optimal double SCB at five different flight conditions.

Note: Cond_i represents ith flight conditions.

Cond_1: $M_\infty = 0.705$, $Cl = 0.690$, $Re = 18.63 \times 10^6$

Cond_2: $M_\infty = 0.730$, $Cl = 0.560$, $Re = 18.63 \times 10^6$

Cond_3: $M_\infty = 0.750$, $Cl = 0.430$, $Re = 18.63 \times 10^6$

Cond_4: $M_\infty = 0.775$, $Cl = 0.300$, $Re = 18.63 \times 10^6$

Cond_5: $M_\infty = 0.800$, $Cl = 0.175$, $Re = 18.63 \times 10^6$

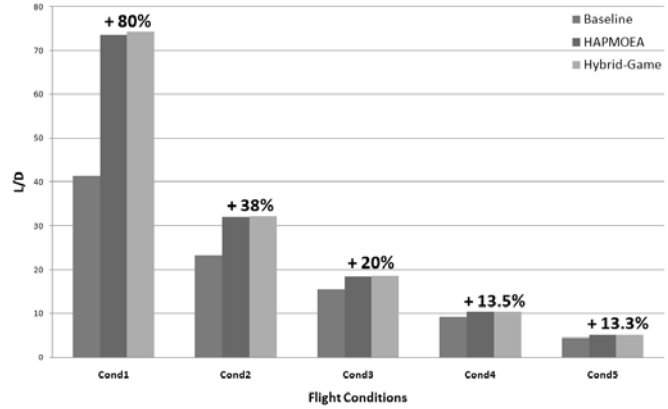

Fig. 18 (b). *L/D* obtained by the optimal double SCB at five different flight conditions.

One example (Cond_1) is shown in Figures 19 (a) and 19 (b) where the pressure ratio contours obtained by the baseline design and with the optimal double SCB solution from the Hybrid-Game are illustrated. Even though the double SCB is optimized at the critical flight condition, the optimal double SCB moves the normal strong shock shown in Figure 19 (a) towards to the trailing edge by 10%c and reduce total drag by 44% which leads to 80% improvement of *L/D*.

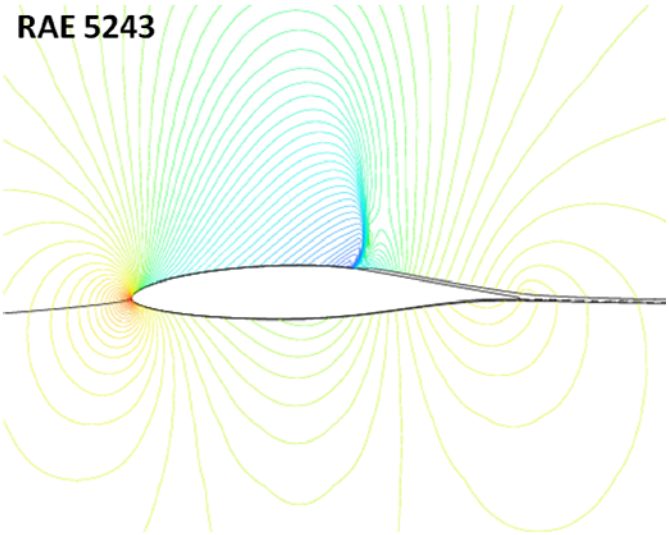

Fig. 19 (a). P/P_0 contour of baseline design at $Cond_1$ (Fig. 18 a)).

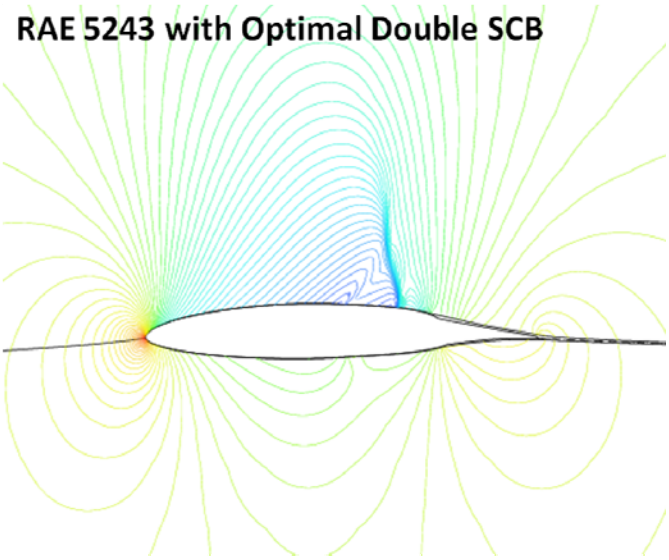

Fig. 19 (b). P/P_0 contour of the optimal double SCB solution obtained by Hybrid-Game at $Cond_1$ (Fig. 18 a)).

To summaries the optimisation test case, double SCB on RAE 5243 is optimised using HAPMOEA and Hybrid-Game to reduce transonic drag at the critical flight conditions. The use of optimal double SCB is beneficial at both normal and critical flow conditions. In addition, Hybrid-Game significantly reduces the computational cost for double SCB design optimisation while generating high quality optimal solution when compared to HAPMOEA.

The design engineer will choose the optimal double SCB obtained by Hybrid-Game which has 10% shorter length than SCB from HAPMOEA. In other words, the double SCB from Hybrid-Game will require less modification in current manufacturing system as well as less material.

6. Conclusion

In this paper, two advanced optimisation techniques have been demonstrated and implemented as a methodology for active flow control bump named Shock Control Bump shape design optimisation. Analytical research clearly shows the benefits of using Hybrid-Game in terms of computational cost and design quality. In addition, the use of SCB on current aerofoil reduces significantly transonic drag. In long term view, the use of SCB will save not only operating cost but also critical aircraft emissions due to less fuel burn.

Future work will focus on robust multi-objective design optimization of SCB (Taguchi method) which can produce the model with better performance and stability at variability of operating conditions and transition positions. In forthcoming research, other evolutionary optimiser including Strength Pareto Evolutionary Algorithm 2 (SPEA2), Self-adaptive Pareto Differential Evolution (SPDE) will be hybridized with Nash-Game strategy and their results will be compared in terms of solution quality and computational cost.

Acknowledgements
The authors gratefully acknowledge E. J. Whitney, and M. Sefrioui, Dassault Aviation for fruitful discussions on Hierarchical EAs and their contribution to the optimisation procedure and, also to M. Drela at MIT for providing *MSES* software. The authors would like to thank Ning Qin at Univ. Sheffield for fruitful discussion on Shock Control Bump.
This work has been supported by the Spanish Ministerio de Ciencia e Innovación through project DPI2008-05250.

References

[1] Lee, D. S., Periaux, J., and Gonzalez, L. F. UAS Mission Path Planning System (MPPS) Using Hybrid-Game Coupled To Multi-Objective Optimiser. *Journal of Dynamic Systems, Measurement and Control*, DS-09-1135. (In Press)
[2] Deb, K., Agrawal, S., Pratap, A., and Meyarivan, T. A fast and elitist multi-objective genetic algorithm: NSGA-II. IEEE Transactions on Evolutionary Computation, 6(2):182–197, 2002.
[3] Lee, D. S., Gonzalez, L. F., Periaux, J., and Srinivas, K., Hybrid-Game Strategies Coupled to Evolutionary Algorithms for Robust Multidisciplinary Design Optimization in Aerospace Engineering. *IEEE Trans. Evolutionary Computation*, TEVC-00213-2009. (In Press)
[4] Periaux, J., Lee, D. S., Gonzalez, L. F., and Srinivas, K. Fast Reconstruction of Aerodynamic Shapes using Evolutionary Algorithms and Virtual Nash Strategies in a CFD Design Environment, *Special Issue Journal of Computational and Applied Mathematics* (JCAM). Vol. 232. Issue 1, pages 61-71, ISSN 0377-0427, 2009.
[5] Lee, D. S., Gonzalez, L. F., and Whitney, E. J. Multi-objective, Multidisciplinary Multi-fidelity Design tool: HAPMOEA – User Guide, Appendix–I, D.S. Lee, Uncertainty Based Multiobjective and Multidisciplinary Design Optimization in Aerospace Engineering, The Univ. of Sydney, Sydney, NSW, Australia. 2007.
[6] Bart-Smith, H., and Risseeuw, P. E. High Authority Morphing Structures, in Proceedings of IMECE 03, no. IMECE 2003-43377, (Washington, D.C), 2003 ASME International Mechanical Engineering Congress, November 2003.
[7] Oborn, R., Kota, S., and Hetrick, J. A. Active Flow Control Using High-Frequency Compliant Structures. *Journal of Aircraft*, Vol. 41, No. 3, pp 603-609. 2004.
[8] Ashill, P. R., Fulker, L. J., and Shires, A. A novel technique for controlling shock strength of laminar-flow aerofoil sections. Proceedings 1st Europian Forum on Laminar Flow Technology, pp. 175-183, Hamburg, Germany, DGLR, AAAF, RAeS, March 16-18 1992.
[9] Qin, N., Zhu, Y., and Shaw, S. T., Numerical Study of Active Shock Control for Transonic aerodynamics, *International Journal of Numerical Methods for Heat & Fluid Flow*, Vol. 14 No. 4, pp 444 – 466, 2004.
[10] Fulker, J. L., and Simmons, M. J. An experiment study of shock control methods, DRA/AS/HWA/TR94007/1, Technical Report, DERA 1994.
[11] An Open Database Workshop for Multiphysics Software Validation, TA5: Shock Control Bump Optimisation On A Transonic Laminar Flow Airfoil. (Chairman N. Qin). Univ. Jyvaskyla, Finland, December 18, 2009 & March 10-12, 2010.
[12] Hansen, N., Ostermeier, A. Completely Derandomized Self-Adaptation in Evolution Strategies. Evolutionary Computation, 9(2), pp. 159-195, 2001.
[13] Hansen, N., Müller, S. D., Koumoutsakos, P. Reducing the Time Complexity of the Derandomized Evolution Strategy with Covariance Matrix Adaptation (CMA-ES). Evolutionary Computation, 11(1), pp. 1-18, 2003.
[14] Wakunda, J., and Zell, A. Median-selection for parallel steady-state evolution strategies. In Marc Schoenauer, Kalyanmoy Deb, Günter Rudolph, Xin Yao, Evelyne Lutton, Juan Julian Merelo, and Hans-Paul Schwefel, editors, ParallelProblem Solving from Nature – PPSN VI, pages 405–414, Berlin, Springer, 2000.
[15] Van Veldhuizen, D. A., Zydallis, J. B. and Lamont, G. B. Considerations in Engineering Parallel Multiobjective Evolutionary Algorithms, IEEE Transactions on Evolutionary Computation, Vol. 7, No. 2, pp. 144-17, 2003.
[16] Sefrioui, M., and Périaux, J. A Hierarchical Genetic Algorithm Using Multiple Models for Optimization. In M. Schoenauer, K. Deb, G. Rudolph, X. Yao, E. Lutton, J.J. Merelo and H.-P. Schwefel, editors, Parallel Problem Solving from Nature, PPSN VI, pages 879-888, Springer, 2000.
[17] Lee, D. S. *Uncertainty Based Multiobjective and Multidisciplinary Design Optimization in Aerospace Engineering*, The Univ. of Sydney, Sydney, NSW, Australia, Section 10.7, p.p. 348-370, 2008.

[18] Zitzler, E., Deb, K., and Thiele, L. Comparison of multiobjective evolutionary algorithms: Empirical results. *Evolutionary Computation*, Vol. 8, (2):173–195, 2000.
[19] Drela, M. A User's Guide to MSES 2.95. MIT Computational Aerospace Sciences Laboratory, September 1996.